Elastic wavefield imaging using the energy norm

Daniel Rocha[1]*, Nicolay Tanushev*[2] *& Paul Sava*[1]
[1]*Center for Wave Phenomena, Colorado School of Mines, and* [2]*Z-Terra, Inc.*

SUMMARY

From the elastic wave equation and the energy conservation principle, we derive a new imaging condition for elastic wavefields. This imaging condition outputs a single image representing the total reflection energy and contains individual terms related to the kinetic and strain energy of the extrapolated wavefields. An advantage of the proposed imaging condition compared to alternatives is that it does not suffer from polarity reversal at normal incidence. This imaging condition also accounts for the directionality of the wavefields in space and time and can be adapted for attenuation of backscattering artifacts in elastic reverse-time migration. Numerical experiments show the quality of energy images compared to conventional counterparts, and the effectiveness of the imaging condition in attenuating backscattering artifacts.

INTRODUCTION

Seismic wavefield imaging is usually implemented using the acoustic wave equation, based on the inaccurate assumption that only compressional waves propagate in the subsurface. More accurate subsurface information describing, for example, fracture distribution, drives the development of wavefield imaging using the elastic wave equation. Multicomponent seismic recording and improved computer resources have made wavefield elastic imaging possible.

Wave-equation migration consists of two steps: wavefield extrapolation in the subsurface, using data recorded at the surface, and the application of an imaging condition with the purpose of extracting the Earth's reflectivity from wavefields (Clærbout, 1985; Dellinger and Etgen, 1990; Yan and Sava, 2009). If a two-way elastic wave equation is used in the wavefield extrapolation step, followed by an imaging condition representing zero-lag crosscorrelation between the wavefields, the imaging procedure is called elastic reverse time migration (RTM) (Hokstad et al., 1998).

Many elastic imaging conditions have been proposed in recent years (Etgen, 1988; Zhe and Greenhalg, 1997; Yan and Sava, 2007; Yan and Xie, 2010; Duan and Sava, 2014). Correlating the displacement fields for each component of the source and receiver wavefields leads to images with a mix of P and S modes, thus making interpretation challenging. Alternatively, if the displacement wavefields are separated into P and S waves using Helmholtz decomposition, one can correlate specific wave modes from source and receiver wavefields (Etgen, 1988; Yan and Sava, 2007). For both displacement and potential imaging conditions, polarity reversal occurs due to changes in the elastic wavefield polarization. Specifically, converted waves change sign due to the different orientation of P and S polarization vectors in relation to the interface (Balch and Erdermir, 1994). Polarity reversal corrections can be done either after angle-domain imaging (Yan and Sava, 2008) or by exploiting the relationship between incidence directions and reflector orientation (Duan and Sava, 2014).

Here, we seek an imaging condition that produces an attribute of the Earth's reflectivity into a single image without polarity reversal, thus facilitating interpretation and providing a concise description of the imaged structures. Our imaging condition is derived from the energy conservation principle of an elastic wavefield.

THEORY

For an isotropic medium, we can write a wave equation:

$$\mathbf{U}_{tt} = \left(v_p^2 - v_s^2\right) \nabla \left(\nabla \cdot \mathbf{U}\right) + v_s^2 \nabla^2 \mathbf{U}\,, \tag{1}$$

where $\mathbf{U}\left(e,\mathbf{x},t\right)$ is the elastic wavefield for experiment e, $v_p^2\left(\mathbf{x}\right)$ and $v_s^2\left(\mathbf{x}\right)$ are P and S velocities, respectively. The subscripts t indicate time derivative. In order to obtain the energy conservation expression for elastic wavefields, we apply the dot product between the elastic wave equation and $\mathbf{U}_t$:

$$\mathbf{U}_t \cdot \mathbf{U}_{tt} = \left(v_p^2 - v_s^2\right) \mathbf{U}_t \cdot \nabla \left(\nabla \cdot \mathbf{U}\right) + v_s^2 \mathbf{U}_t \cdot \nabla^2 \mathbf{U}\,. \tag{2}$$

Rearranging the left-hand side by the chain rule and integrating all terms over the whole spatial domain Ω, we obtain

$$\begin{aligned} \frac{1}{2}\frac{d}{dt}\int_\Omega |\mathbf{U}_t|^2 \, d\mathbf{x} &= \int_\Omega \left(v_p^2 - v_s^2\right) \mathbf{U}_t \cdot \nabla \left(\nabla \cdot \mathbf{U}\right) d\mathbf{x} \\ &+ \int_\Omega v_s^2 \mathbf{U}_t \cdot \nabla^2 \mathbf{U} \, d\mathbf{x}\,. \end{aligned} \tag{3}$$

We can develop the two terms on the right-hand side of equation 3 separately. For the first term, using integration by parts and then divergence theorem, we obtain

$$\begin{aligned} &\int_\Omega \left(v_p^2 - v_s^2\right) \mathbf{U}_t \cdot \nabla \left(\nabla \cdot \mathbf{U}\right) d\mathbf{x} \\ &= -\int_\Omega \left(v_p^2 - v_s^2\right) \left(\nabla \cdot \mathbf{U}_t\right) \left(\nabla \cdot \mathbf{U}\right) d\mathbf{x} \qquad (4) \\ &= -\frac{1}{2}\frac{d}{dt}\int_\Omega \left(v_p^2 - v_s^2\right) |\nabla \cdot \mathbf{U}|^2 \, d\mathbf{x}\,. \qquad (5) \end{aligned}$$

Similarly, for the second term on the right-hand side of equation 3, we use the component-wise application of the Laplacian operator ∇^2 on the vector field $\mathbf{U}$. Then, the application of the dot product leads to the sum of three terms in the form $b_t \nabla^2 b$. For each component of the wavefield, using the Green's

first identity, the dot product on the right-hand side becomes a Frobenius product:

$$\begin{aligned}
&\int_\Omega v_s^2 \mathbf{U}_t \cdot \nabla^2 \mathbf{U}\, d\mathbf{x} \\
&= -\int_\Omega \left(\nabla\left(v_s^2 \mathbf{U}_t\right)\right) : (\nabla \mathbf{U})\, d\mathbf{x} \qquad (6)\\
&= \int_\Omega v_s^2 (\nabla \mathbf{U}_t) : (\nabla \mathbf{U})\, d\mathbf{x} \qquad (7)\\
&= \frac{1}{2}\frac{d}{dt}\int_\Omega v_s^2 \|\nabla \mathbf{U}\|_F^2 d\mathbf{x}, \qquad (8)
\end{aligned}$$

where $\|\cdot\|_F^2$ is the Frobenius norm.

Then, equation 3 can be written as

$$\frac{1}{2}\frac{d}{dt}\int_\Omega \left(|\mathbf{U}_t|^2 + \left(v_p^2 - v_s^2\right)|\nabla\cdot\mathbf{U}|^2 + v_s^2\|\nabla\mathbf{U}\|_F^2\right) d\mathbf{x} = 0\,. \qquad (9)$$

Equation 9 is in the form $\dot{E}(t) = 0$. Therefore, the function E measures the total energy of the wavefield within a domain:

$$E(t) = \int_\Omega \left(|\mathbf{U}_t|^2 + \left(v_p^2 - v_s^2\right)|\nabla\cdot\mathbf{U}|^2 + v_s^2\|\nabla\mathbf{U}\|_F^2\right) d\mathbf{x}\,. \qquad (10)$$

Equation 10 represents the total mechanical energy function in terms of kinetic and potential energies at every point in space and at all times. The first term, composed of particle velocity, represents the wavefield kinetic energy (Holstrom, 1968). Under the assumption that the total energy is conserved, the remaining terms of equation 10 can be interpreted as potential energy:

- The $\nabla\cdot\mathbf{U}$ term captures the volumetric strain of the elastic medium deforming under the influence of a passing wave
- The $\|\nabla\mathbf{U}\|_F$ term captures, among other things, the torsional deformation of the elastic solid

Defining equation 10 as the energy norm of a wavefield, we can also define an inner product between wavefields $\mathbf{U}$ and $\mathbf{V}$:

$$<\mathbf{U},\mathbf{V}>_E \equiv \mathbf{U}_t\cdot\mathbf{V}_t + \left(v_p^2 - v_s^2\right)(\nabla\cdot\mathbf{U})(\nabla\cdot\mathbf{V}) + v_s^2\,(\nabla\mathbf{U}):(\nabla\mathbf{V})\,. \qquad (11)$$

IMAGING CONDITION

We propose a new elastic imaging condition based on the inner product in equation 11 between source and receiver wavefields, followed by integration over time:

$$I_E = \sum_{e,t} \mathbf{U}_t\cdot\mathbf{V}_t + \left(v_p^2 - v_s^2\right)(\nabla\cdot\mathbf{U})(\nabla\cdot\mathbf{V}) + v_s^2\;(\nabla\mathbf{U}):(\nabla\mathbf{V})\,. \qquad (12)$$

Here, $\mathbf{U}(e,\mathbf{x},t)$ and $\mathbf{V}(e,\mathbf{x},t)$ are the source and receiver vector wavefields, respectively, and $I_E(\mathbf{x})$ is the scalar energy image. We can describe this imaging condition as a dot product between the following multidimensional vectors:

$$\begin{aligned}
\square\mathbf{U} &= \left\{\mathbf{U}_t, \sqrt{v_p^2 - v_s^2}\,(\nabla\cdot\mathbf{U}), v_s\,(\nabla\mathbf{U})\right\}, \qquad (13)\\
\square\mathbf{V} &= \left\{\mathbf{V}_t, \sqrt{v_p^2 - v_s^2}\,(\nabla\cdot\mathbf{V}), v_s\,(\nabla\mathbf{V})\right\}. \qquad (14)
\end{aligned}$$

Equations 13 and 14 define multidimensional vectors with thirteen components, of which three components are the wavefield time derivatives $(\mathbf{U}_t, \mathbf{V}_t)$, one is the scaled divergence of the wavefields $(\nabla\cdot\mathbf{U}, \nabla\cdot\mathbf{V})$, and nine are from the tensor wavefield gradient $(\nabla\mathbf{U}, \nabla\mathbf{V})$.

Therefore, we can rewrite the imaging condition equation 12 as

$$I_E = \sum_{e,t} \square\mathbf{U}\cdot\square\mathbf{V}\,. \qquad (15)$$

This expression is analogous to the similar imaging condition developed for acoustic wavefields (Rocha et al., 2015), and has similar physical interpretation and application.

Vectors $\square\mathbf{U}$ and $\square\mathbf{V}$ are related to the polarization and propagation directions of the elastic wavefields $\mathbf{U}$ and $\mathbf{V}$. Decomposing the wavefield $\mathbf{U}$ in plane waves, we obtain

$$\mathbf{U} = \mathbf{u}_0 e^{i\omega(\mathbf{p}\cdot\mathbf{x} - t)}\,, \qquad (16)$$

where $\mathbf{u}_0$ is the polarization vector, $\mathbf{p}$ is the slowness vector, and ω is the frequency. We assume that ω is large and that the vectors $\mathbf{u}_0$ and $\mathbf{p}$ are slowly varying in space and time, which makes the spatial and temporal derivatives of $\mathbf{u}_0$ and $\mathbf{p}$ small compared to ω. Substituting the plane wave definition, equation 16, into the solution of the elastic equation 1, we obtain the Christoffel equation for isotropic media:

$$\mathbf{u}_0 = \left(v_p^2 - v_s^2\right)(\mathbf{u}_0\cdot\mathbf{p})\,\mathbf{p} + v_s^2\,(\mathbf{p}\cdot\mathbf{p})\,\mathbf{u}_0\,. \qquad (17)$$

Multiplying equation 17 by $\mathbf{u}_0$ leads to

$$|\mathbf{u}_0|^2 = \left(v_p^2 - v_s^2\right)(\mathbf{u}_0\cdot\mathbf{p})^2 + v_s^2|\mathbf{p}|^2|\mathbf{u}_0|^2\,. \qquad (18)$$

The terms in the vectors $\square\mathbf{U}$ and $\square\mathbf{V}$ are also in function of the polarization and slowness vectors $\mathbf{u}_0$ and $\mathbf{p}$:

$$\begin{aligned}
\mathbf{U}_t &= -i\omega\mathbf{u}_0 e^{i\omega(\mathbf{p}\cdot\mathbf{x} - t)}\,, \qquad (19)\\
\nabla\cdot\mathbf{U} &= i\omega\,(\mathbf{u}_0\cdot\mathbf{p})\,e^{i\omega(\mathbf{p}\cdot\mathbf{x} - t)}\,, \qquad (20)\\
\nabla\mathbf{U} &= -i\omega\,(\mathbf{u}_0\otimes\mathbf{p})\,e^{i\omega(\mathbf{p}\cdot\mathbf{x} - t)}\,, \qquad (21)
\end{aligned}$$

where $\otimes$ indicates the outer product between two vectors, resulting in a matrix.

We seek to define an imaging condition that attenuates waves propagating along the same path and with the same polarization, i.e., elastic backscattering. Defining $(\square\mathbf{V})^\dagger$ as

$$(\square\mathbf{V})^\dagger = \left\{-\mathbf{V}_t, \sqrt{v_p^2 - v_s^2}\,(\nabla\cdot\mathbf{V}), v_s\,(\nabla\mathbf{V})\right\}, \qquad (22)$$

we compute the dot product between $\square\mathbf{U}$ and $(\square\mathbf{V})^\dagger$ as

$$\square\mathbf{U}\cdot(\square\mathbf{V})^\dagger = \qquad (23)$$
$$\omega^2\left[|\mathbf{u}_0|^2 - \left(v_p^2 - v_s^2\right)(\mathbf{u}_0\cdot\mathbf{p})^2 + v_s^2|\mathbf{p}|^2|\mathbf{u}_0|^2\right] e^{i\omega(\mathbf{p}\cdot\mathbf{x} - t)}\,.$$

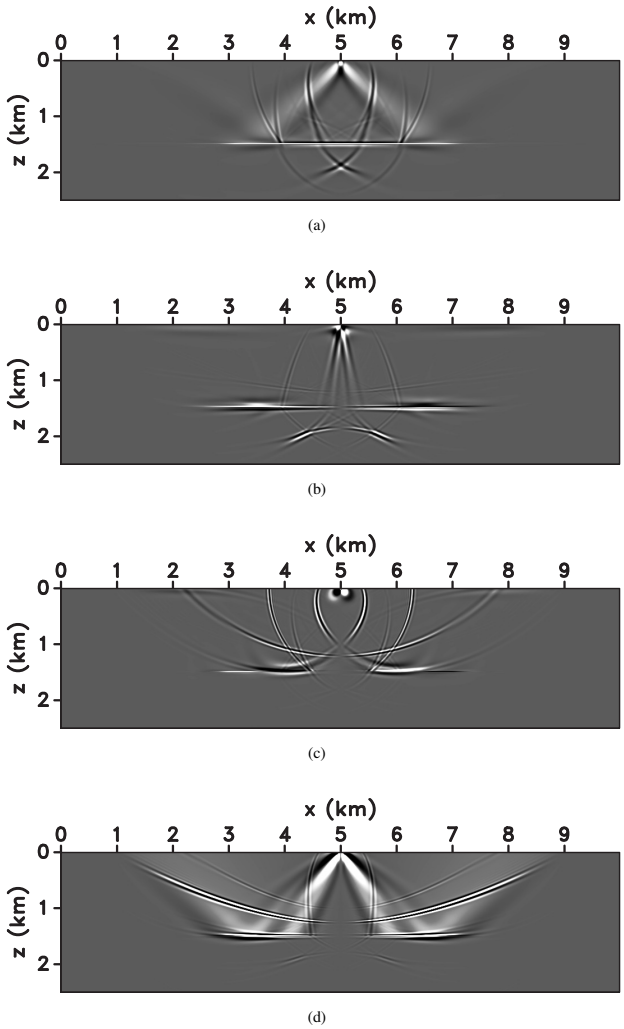

Figure 1: Images with scalar and vector potentials: (a) PP, (b) PS, (c) SP and (d) SS. Note that backscattering artifacts do not occur in (b) and (c) due to correlation of different wave modes.

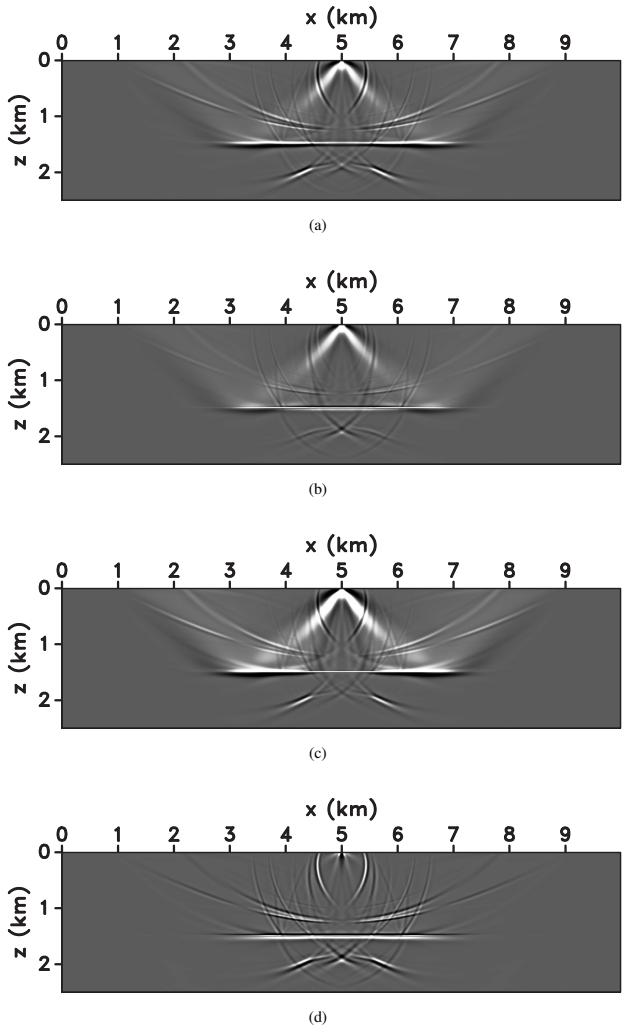

Figure 2: (a) Kinetic and (b) potential energy images; total energy image (c) with and (d) without backscattering.

Using the relation 18, we obtain

$$\Box\mathbf{U}\cdot(\Box\mathbf{V})^{\dagger}=0\,, \tag{24}$$

i.e., the dot product is zero everywhere except at locations where reflectors exist or different wave modes interact, since the vectors $\mathbf{p}$ and $\mathbf{u}_0$ are different for $\mathbf{U}$ and $\mathbf{V}$ at these locations. Therefore, the dot product in equation 24 nullifies the waves that propagate on the same path and have the same polarization. Such events include reflection backscattering, diving waves, direct and head waves from the same wave modes. Therefore, the imaging condition

$$I_E^{\dagger}=\sum_{e,t}\Box\mathbf{U}\cdot(\Box\mathbf{V})^{\dagger} \tag{25}$$

attenuates backscattering artifacts in elastic RTM images.

EXAMPLES

Using a simple model with a horizontal reflector at $z=1.5$km, we test the proposed imaging condition and compare it with its conventional counterparts in Figures 1 and 2. We also include a reflector in the migration velocity that causes backscattering artifacts. In the PS (Figure 1b) and SP (Figure 1c) images, the converted reflections do not correlate with the incident waves, thus freeing these images from backscattering artifacts. The energy imaging condition also shows backscattering artifacts (Figure 2c). However, using the modified energy imaging condition in equation 25, we attenuate the backscattering artifacts (Figure 2d).

Figures 3a and 3b show elastic energy images for the Marmousi model. Using the energy imaging condition in equation 12, we obtain the image in Figure 3a, which presents backscattering artifacts. We attenuate these artifacts in Figure 3b using the imaging condition from equation 25. The individual elastic images for shots do not show polarity rever-

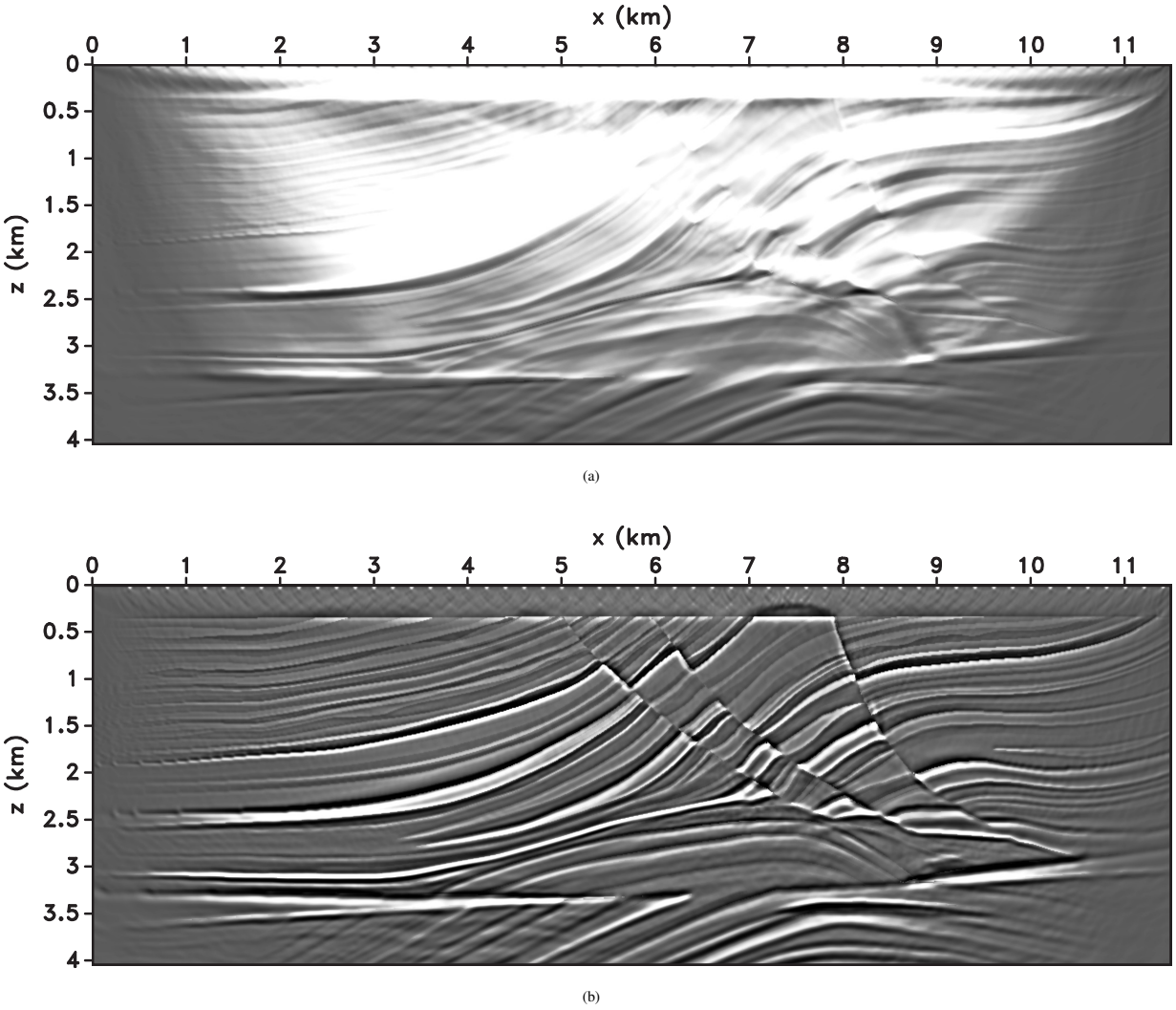

Figure 3: Marmousi elastic migration with the energy imaging condition. Energy image using (a) imaging condition equation 15, and (b) imaging condition equation 25. The image in (b) shows no artifacts from polarity reversal and attenuated backscattering energy compared to (a).

sal at normal incidence, and therefore, stacking is constructive, leading to a good quality image, as seen in Figure 3b.

CONCLUSIONS

The energy imaging condition offers an alternative to conventional elastic imaging conditions, which use potentials or displacement components. This alternative combines all wave modes into a single image and does not suffer from polarity reversal, as is the case for conventional images using converted modes, either with potentials or displacements. The energy imaging condition accounts for wavefield directionality, including the wavefield propagation and polarization directions. We describe this imaging condition as the projection between the multidimensional vectors $\Box\mathbf{U}$ and $\Box\mathbf{V}$ (built using the extrapolated wavefields $\mathbf{U}$ and $\mathbf{V}$), whose terms contain information about wavefield directionality. By exploiting the wavefield directionality, we are able to attenuate the backscattering artifacts in elastic images, without making use of artificial low-pass (e.g. Laplacian) filters.

ACKNOWLEDGMENTS

We would like to thank sponsor companies of the Consortium Project on Seismic Inverse Methods for Complex Structures, whose support made this research possible. We acknowledge Yuting Duan, who provided the elastic modeling code for this research. The reproducible numeric examples in this paper use the Madagascar open-source software package (Fomel et al., 2013) freely available from http://www.ahay.org.

REFERENCES

Balch, A. H., and C. Erdermir, 1994, Sign-change correction for prestack migration of P-S converted wave reflections: Geophysical Prospecting, **42**, 637–663.

Clærbout, J. F., 1985, Imaging the Earth's Interior: Blackwell Scientific Publications.

Dellinger, J., and J. Etgen, 1990, Wave-field separation in two-dimensional anisotropic media: Geophysics, **55**, 914–919.

Duan, Y., and P. Sava, 2014, Converted-waves imaging condition for elastic reverse-time migration: Presented at the SEG 2014 Denver Annual Meeting.

Etgen, J. T., 1988, Prestacked migration of P- and SV-waves: Presented at the SEG 1988 Annual Meeting.

Fomel, S., P. Sava, I. Vlad, Y. Liu, and V. Bashkardin, 2013, Madagascar: open-source software project for multidimensional data analysis and reproducible computational experiments: Journal of Open Research Software, **1**.

Hokstad, K., R. Mittet, and M. Landrø, 1998, Elastic reverse time migration of marine walkaway vertical seismic profiling data: Geophysics, **63**, 1685–1695.

Holstrom, G., 1968, Nonlinear energy transfer in elastic waves: Geophysics, **33**, 734–746.

Rocha, D., N. Tanushev, and P. Sava, 2015, Acoustic wavefield imaging using the energy norm: Presented at the SEG 2015 New Orleans Annual Meeting.

Yan, J., and P. Sava, 2007, Elastic wavefield imaging with scalar and vector potentials: Presented at the SEG Denver 2007 Annual Meeting.

———, 2008, Isotropic angle-domain elastic reverse-time migration: Geophysics, **73**, S229–S239.

———, 2009, Elastic wave-mode separation for VTI media: Geophysics, **74**, WB19–WB32.

Yan, R., and X.-B. Xie, 2010, The new angle-domain imaging condition for elastic RTM: Presented at the SEG Denver 2010 Annual Meeting.

Zhe, J., and S. A. Greenhalg, 1997, Prestack multicomponent migration: Geophysics, **62**, 598–613.